JOURNAL OF CATALYSIS 117, 549–557 (1989)

Gasification of Graphite by the Channeling Action of Metal Catalysts

JOHN A. TSAMOPOULOS,[1] HEMANT W. DANDEKAR, AND JAN H. SCHOLTZ

Department of Chemical Engineering, State University of New York, Buffalo, New York 14260

Received November 22, 1988; revised January 23, 1989

The channeling action of metal catalysts during graphite gasification is studied. A comprehensive model is developed using all available data in the literature. The dependence of the channeling velocity on the inverse of the particle diameter under oxidation over Pd is shown to be due to slower diffusion of carbon atoms through the catalyst bulk. On the other hand the proportionality of the channel propagation rate to the surface area of the particle available for reaction under hydrogenation over Ni is shown to be due to a slower surface reaction. In both cases increase of the channel depth retards the motion of the catalytic particle.

INTRODUCTION

Over the last 25 years, considerable work has been done in the field of catalytic oxidation or reduction of graphite using as catalysts over 40 metals, metal oxides, and salts. The effects of nickel, platinum, palladium, iron, copper, and other transition metals have been studied and possible reaction mechanisms have been proposed as summarized in the review articles by Walker *et al.* (*1*) and McKee (*2*). The oxidizing reactants have been combinations of oxygen, steam, and carbon dioxide, whereas the reducing medium has usually been hydrogen. Most of these studies were experimental in nature and provided considerable insight in understanding the complex phenomena that take place during this process. However, a number of unanswered questions which continue to hold the interest of the scientific community remain.

During gasification the active catalytic particles were observed to continuously translate in order to remain in contact with new portions of the substrate carbon. Depending on the position and motion of the catalyst this action has been called mono- or multilayer channeling, tunneling, pitting, or edge recession. The most commonly encountered action is channeling; the particle produces a channel that is several graphite layers deep and translates parallel to the carbon basal planes at a constant speed. This is the action that will be studied here and only the most relevant and recent results will be summarized next.

Baker *et al.* (*3*) studied catalytic oxidation of graphite by platinum and palladium using controlled atmosphere electron microscopy (CAEM). This technique has been introduced and refined by Baker and co-workers (see, for example, Baker (*4*)) and allows for continuous observation of the catalyst while gasification is taking place. However, it does not provide information about the absolute value of the depth of the channels or the dimensions of the catalyst except for its projected area. Quantitative analysis of their results indicated that the linear channeling rate is inversely proportional to the depth of the channel as well as to the particle size for particles cutting channels of similar depth.

Baker and Sherwood (*5*) investigated the catalytic gasification of graphite by nickel in various gaseous environments. Under strong oxidizing conditions, gasification occurred mainly by the uncatalyzed route. Under milder steam/O_2 environments, catalyzed and uncatalyzed reactions were found to occur at comparable rates. In contrast to this, the reduction of graphite by H_2

[1] To whom correspondence should be addressed.

0021-9517/89 $3.00

took place mainly by the catalyzed route. No pitting was observed in either case. While the channeling rate, for reduction by H_2 over Ni, was found to be proportional to the square of the particle diameter, it was inversely proportional to it for oxidation by steam/O_2. This suggests fundamental differences in the mechanisms for the two reactions. Nevertheless, care must be taken in analyzing the oxidation results due to the fact that they are contaminated by the products from the uncatalyzed route and the metal particles may have been transformed to NiO.

The catalytic reduction of graphite in the presence of Ni has also been studied by Keep *et al.* (*6*). The linear rate was similarly observed to be proportional to the particle area. The suggested mechanisms were that the catalyst acts like a dissociation center for either hydrogen or carbon which subsequently diffuses through its bulk and reacts on the rest of the interface with carbon or hydrogen, respectively. A direct consequence of such a mechanism would be that the rate of gasification would be inversely proportional to the particle size, if bulk diffusion is the rate-limiting step, whereas it would be proportional to the available surface area for reaction, if surface reaction is the rate-limiting step.

In addition, Goethel and Yang (*7*) studied monolayer channeling on the basal planes of graphite for the platinum-catalyzed C–H_2 reaction. They used a combination of transmission electron microscopy (TEM) and gold decoration of the substrate to make visible the single-layer steps. Thus, they obtained accurate measurements of the channel depth and width, but not during the channeling action. From the overall kinetic data they concluded that surface reaction between adsorbed H_2 and dissolved-in-platinum carbon was controlling, since the rate of channeling was directly proportional to the particle surface area.

Recently, Choi *et al.* (*8*) have presented a model for the oxidation of graphite with oxygen using a platinum catalyst. The catalyst was modeled as a cube into which carbon entered only through the front face and reacted only on the top face, where a thin oxide layer was formed. Despite the fact that reaction was not allowed to take place in the rear face, that diffusion coefficients were estimated from data for nitrogen on tungsten, and that diffusion coefficients of carbon atoms through metals and metal oxides should be different, good agreement was obtained with rate measurements by adjusting only one constant.

The present study is aimed at gaining further insight into the interplay between diffusion and surface reaction and the various parameters (physical, chemical, and geometrical) which affect the channeling rate under either a reducing or an oxidizing environment. However, given the complexities of the problem associated with unexplained phenomena at the metal–carbon interface (e.g., the fluid-like behavior of the particle and the importance of adhesion forces for sustaining the motion of the particle), certain simplifying assumptions will be made.

MODEL DESCRIPTION AND SOLUTION PROCEDURE

It is now generally thought that the channeling action (both deep and monolayer) occurs in four major steps. First, carbon from the substrate must be activated on the metal surface and is assumed to take some carbidic form or to dissolve in the metal (i.e., carbon–carbon bonds must be broken and carbon–metal bonds must be formed). Second, these carbon atoms must be transferred through the metal matrix toward the metal surface exposed to the gasifying gas. Third, the reactant gas must be activated on the metal surface and undergo reaction with the carbon atoms. Finally, the products must be desorbed.

Due to the small size of the catalyst, its high values of conductivity, and the small channeling velocity, temperature gradients inside it are not established even for highly exothermic and endothermic reactions

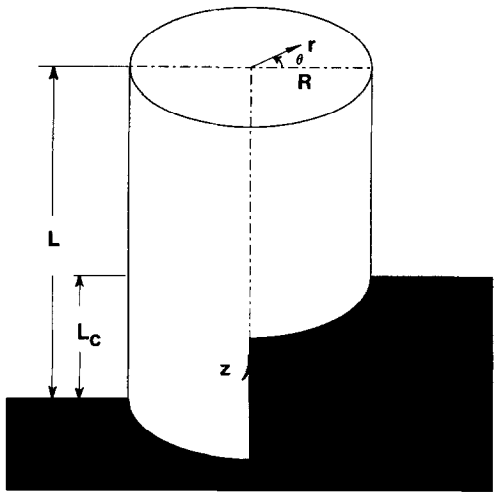

FIG. 1. Schematic representation of a metal particle of radius R, height L forming a channel of depth L_c.

(Holstein and Boudart (*9*)), in contrast to some initial suggestions for the opposite. Even when the surface reaction is rate controlling, H_2 concentration does not influence it (Baker and Sherwood (*5*)). Thus, the reaction rate is taken to be only first order in carbon, and the reaction takes place in all exposed surfaces of the particle.

The particle shape and size vary depending on the reactant gases and operating temperature. Both cylindrical and semispherical particles have been observed and are considered to be more realistic than cubic ones used elsewhere (Choi *et al.* (*8*), Goethel *et al.* (*10*)). A particle of cylindrical shape that remains unchanged during the process and forms a channel of constant but arbitrary depth on the surface basal plane is assumed here (Fig. 1). The variation introduced by choosing a semispherical geometry is not believed to be significant and can be readily treated by the same general method.

Since the particle remains undeformed it moves with a uniform velocity in a given direction. This last consequence requires that the flux of carbon through a surface normal to its velocity must not vary. As a result, the flux through the particle at every point on its front surface adjusts accordingly. This in turn suggests that the carbon flux and the linear channeling rate must be set by that point on the particle that provides the longest diffusion length to the reacting surface. Obviously, this point is the bottom-front tip of the particle where it is assumed that the carbon concentration equals the carbon solubility in the metal at the operating temperature, i.e., that there is local equilibrium between the particle and the substrate.

Under the above-mentioned conditions it follows that the concentration of carbon throughout the metal particle is governed by the diffusion equation along with the appropriate boundary conditions on the particle surfaces. With the dimensionless length in the particle defined as $(r, z) = (\bar{r}, \bar{z})/R$, where R is the particle radius, and the dimensionless concentration as $C = \bar{C}/C_0$, where C_0 is the solubility of carbon in the catalyst, these equations are

$$\frac{\partial^2 C}{\partial r^2} + \frac{1}{r}\frac{\partial C}{\partial r} + \frac{1}{r^2}\frac{\partial^2 C}{\partial \theta^2} + \frac{\partial^2 C}{\partial z^2} = 0 \quad (1)$$

$$\frac{\partial C}{\partial z} = 0 \qquad \text{at } z = 0 \quad (2)$$

$$\frac{\partial C}{\partial z} = -DaC \qquad \text{at } z = z_2 \quad (3)$$

$$\frac{\partial C}{\partial r} = -DaC \qquad \text{at } \begin{cases} z_1 \le z \le z_2, & 0 \le \theta \le \pi \\ 0 \le z \le z_1, & \dfrac{\pi}{2} \le \theta \le \pi \end{cases} \quad (4)$$

$$\frac{\partial C}{\partial \theta} = 0 \qquad \text{at } \theta = 0 \text{ and } \theta = \pi \quad (5)$$

$$K = \frac{1}{\cos\theta}\frac{\partial C}{\partial r} \qquad \text{at } 0 \le z \le z_1, \quad 0 \le \theta \le \frac{\pi}{2} \quad (6)$$

$$C = 1 \qquad \text{at } \theta = 0, \quad z = 0, \quad r = 1, \quad (7)$$

where $Da = kR/D$ is the Damkohler num-

ber, k is the first-order reaction rate constant based on the volume concentration of carbon in the particle, D is the diffusivity of carbon in the metal, $z_1 = L_c/R$, $z_2 = L/R$, L_c is the channel depth, and L the particle height. Equation (2) dictates that no pitting takes place and the particle simply moves on a basal plane. Equations (3) and (4) account for the first-order—in carbon concentration—surface reaction taking place in all exposed surfaces of the particle. Equation (5) is a simple consequence of the symmetry in the problem. Equation (6) sets the flux of carbon toward the particle equal to a constant, $K = v\rho R/DMC_0$, everywhere in the covered portion of the particle. In this expression v is the linear velocity of the catalytic particle, ρ its density, and M the molecular weight of carbon. However, this equation is not sufficient as a boundary condition because the linear velocity is not known a priori. Consequently, the constant K will be calculated so that the bottom-front corner of the particle is saturated with carbon as required by Eq. (7).

It should be noted here that setting the carbon concentration everywhere on the front surface equal to its solubility would force the upper portion of the particle to move faster than the lower one in order to simply maintain contact with the more rapidly consumed carbon there. According to the present model, carbon concentration in the front face except for the bottom tip is less than the saturation value and is determined so that Eq. (6) is satisfied.

Common analytical techniques could not be used here to provide a solution, given the complexity of the boundary conditions. Hence, a numerical procedure had to be followed. The equations were solved using the Galerkin/finite element method with three-dimensional linear basis functions. According to this method the particle is divided into subdomains or elements and in each element the concentration is approximated by a low-order polynomial. The coefficients, α_i, of the polynomials, ψ_i, are calculated so that the weighted residuals of the governing equation are zeroed. In this way, the original problem is reduced to a system of algebraic equations for the coefficients of the polynomials. When the weighting functions coincide with the chosen polynomials the Galerkin method results. Since linear Lagrangian polynomials are used, integration by parts of Eq. (1) is necessary. Finally, the algebraic equations to be solved reduce to

$$\iiint_V \left[\psi_i \frac{1}{r}\frac{\partial C}{\partial r} - \frac{\partial \psi_i}{r}\frac{\partial C}{\partial r} - \frac{1}{r^2}\frac{\partial \psi_i}{\partial \theta}\frac{\partial C}{\partial \theta} - \frac{\partial \psi_i}{\partial z}\frac{\partial C}{\partial z}\right] r\,dr\,d\theta\,dz$$

$$+ \int_{\theta=0}^{\theta=\pi/2}\int_{z=0}^{z=z_1} \psi_i K \cos\theta\, d\theta\, dz - \int_{\theta=\pi/2}^{\theta=\pi}\int_{z=0}^{z=z_1} \psi_i Da\, C(r=1)\, d\theta\, dz$$

$$- \int_{\theta=0}^{\theta=\pi}\int_{z=z_1}^{z=z_2} \psi_i Da\, C(r=1)\, d\theta\, dz$$

$$- \int_{\theta=0}^{\theta=\pi}\int_{r=0}^{r=1} \psi_i Da\, C(z=z_2)\, d\theta\, dr = 0. \quad (8)$$

The number of elements in each direction was increased until it was found that 12 elements in each direction led to satisfactory results. In order to confirm this observation a test was made with 18 elements in each direction using the extended addressing capability of the Cornell Theory Center's IBM-3090 and the relative change from the result using a 12-element mesh was found to be about 0.07%. Thus, 12 elements were used for most calculations resulting in 2197 algebraic equations that were solved simultaneously using Gaussian elimination.

RESULTS AND DISCUSSION

The two fundamentally different effects of the particle size on the channeling rate will be examined, namely, the linear increase of the channeling rate with the exposed area of the particle during reduction with H_2/Ni (*6*), and the inverse proportionality of the channeling velocity to the particle diameter during oxidation with O_2/Pd (*3*). The goal is to be able to reproduce the

TABLE 1

Physicochemical and Geometrical Parameters Used for C Oxidation over Pd

Diffusivity	$D = 9.553 \times 10^{-2} \exp\left(-\frac{13{,}744}{T}\right) \frac{cm^2}{s}$ $\left(5.34 \times 10^{-9} \frac{cm^2}{s} \text{ at } 823 \text{ K}\right)$
Solubility	$C_0 = 0.6 \times \exp\left(-\frac{4{,}051}{T}\right) \frac{g}{cm^3}$ $\left(0.0044 \frac{g}{cm^3} \text{ at } 823 \text{ K}\right)$
Particle diameter	$10 \text{ nm} \leq 2R \leq 100 \text{ nm}$
Ratio of particle height to diameter	$L/2R = 1$ and 2
Ratio of channel depth to particle height	$0.1 \leq L_c/L \leq 1.0$

experimental results using all the available physical parameters in the literature and thus provide a predictive model. Since the only missing parameter in either case is the reaction rate constant this is calculated by fitting the model prediction for the channeling velocity to only one experimental point.

The oxidation over Pd is examined first under the conditions summarized in Table 1. The values for diffusivity and solubility of carbon in Pd in the temperature range 500°–600°C have been measured by Goethel (*11*). The reaction rate constant is calculated by fitting the channeling velocity predicted by this model to the experimental value for a particle of diameter 52 nm assuming that its height is equal to its diameter and that the channel depth is half its height. It was found that a better fit for all particle sizes was obtained keeping all other parameters constant, by assuming that the operating temperature is somewhat lower than the one reported by Baker *et al.* (*3*), i.e., 550°C instead of 575°C. The former could have indeed been the actual temperature given the experimental conditions. The temperature was measured by calibration with a set of thermocouples in contact with the heating ribbon (not with the graphite). In addition, cold O_2 was introduced in the reaction chamber making the reported temperatures considerably higher than the actual particle temperatures (C. Lund, private communication).

The resulting reaction rate constant is $k = 2.52 \times 10^{-4}$ cm/s and this value is used for the rest of the oxidation calculations unless otherwise indicated. In Fig. 2, a set of constant concentration surfaces throughout the particle mentioned earlier is shown. This set was produced using a DI-3000 graphics program and interpolating the numerical result. As stated in the previous section, the concentration of carbon is not the same in the external surface exposed to graphite. Its maximum value equals the car-

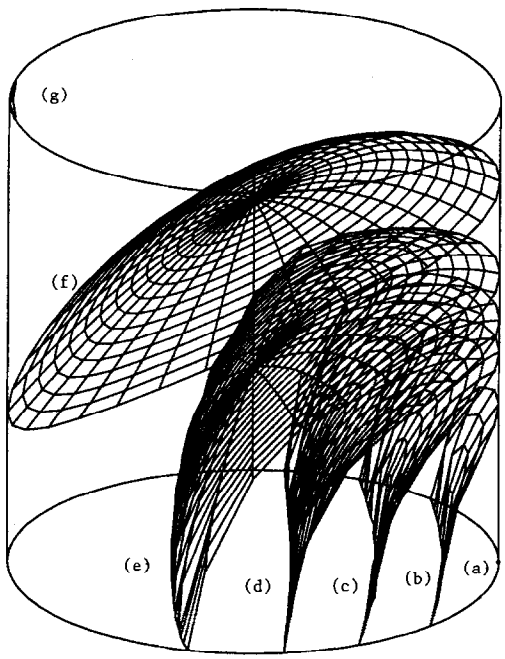

FIG. 2. Planes of constant carbon concentration inside the Pd particle. Geometric parameters: $2R = 52$ nm, $L/2R = 1$, $L_c/L = 0.5$. The different surfaces correspond to carbon concentrations in grams per cubic centimeter of (a) 0.0044, (b) 0.0040, (c) 0.0036, (d) 0.0032, (e) 0.0029, (f) 0.0025, and (g) 0.0021.

bon solubility and is attained in the bottom-front of the particle and continuously decreases as the surface exposed to the oxidizing gas are approached. Indeed, a delicate balance of carbon influx must take place around the front surface of contact between the carbon substrate and the particle. This observation coupled with the fact that at this microscopic level the graphite structure is not really homogeneous may explain the observation by Baker and Sherwood (*5*) that the particle seems to "breathe" and undergo periodic rearrangements in shape during the channeling process. At any rate, the channeling velocity is proportional to carbon solubility as noted by Goethel *et al.* (*10*).

The dependence of channeling velocity on particle diameter is shown in Fig. 3. Two different particle aspect ratios have been considered, $L/2R = 1$ and 2, and 50% coverage of the front surface by graphite ($L_c/L = 0.5$). In order to match Baker's result for a particle diameter of 52 nm the reaction rate constant for aspect ratio $L/2R = 2$ must be increased to $k = 5.99 \times 10^{-4}$ cm/s, from the previously used value. According to this figure the channeling velocity decreases as the particle diameter increases, but in a manner that depends on the particle aspect ratio. Generally, increasing the particle size increases the diffusion path that carbon atoms must cover in order to reach the surface on which reaction takes place. Thus, Fig. 3 indicates that carbon diffusion through the bulk of the catalyst is much slower than its oxidation on the palladium surface and controls the phenomenon.

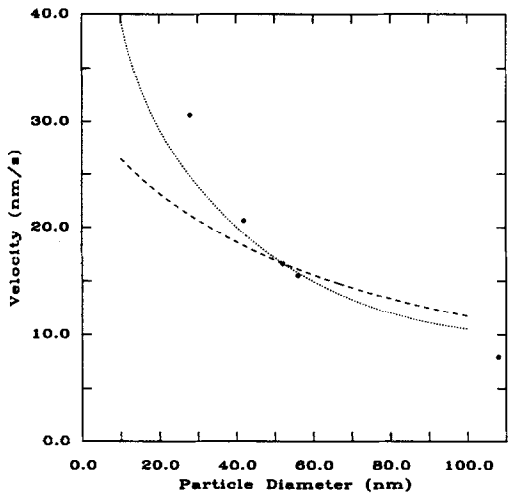

FIG. 3. Predicted values for 50% particle coverage and experimental results by Baker *et al.* (*3*) for particle velocity during oxidation of graphite over Pd. (---) $L/2R = 1$ and $k = 2.52 \times 10^{-4}$ cm/s; (· · ·) $L/2R = 2$ and $k = 5.99 \times 10^{-4}$ cm/s; (•••) experimental data.

Consistent with this explanation are the following two effects due to variations in aspect ratio. First, larger aspect ratio means that the average diffusion path in the particle has increased even for particles of the same diameter. Consequently, for the overall rate to remain unchanged for a particle diameter of 52 nm the reaction rate constant must be increased, as noted earlier. Second, when the aspect ratio is different, varying the particle size will affect differently the diffusion path inside the particle. For example, the distance between the lower point in the front of the particle (the point saturated with carbon) and the upper point in the back of the particle (the point with the minimum carbon concentration) increases by a factor of $\sqrt{2}n$ for $L/2R = 1$ and by a factor of $\sqrt{5}n$ for $L/2R = 2$, for an n-fold increase in the diameter. Therefore, the velocity for a particle of larger aspect ratio shows a more dramatic decrease as the particle size increases. Finally, as noted in Fig. 2 the side surface of the particle has a higher carbon concentration than the top resulting in larger consumption of carbon there, which further increases when the aspect ratio increases.

The experimental results by Baker *et al.* (*3*) are also shown in Fig. 3 and do not exactly coincide with either of the curves. However, in that paper no indication of the exact particle height or channel depth is given because the CAEM technique provided only a two-dimensional view. The present analysis makes clear that the chan-

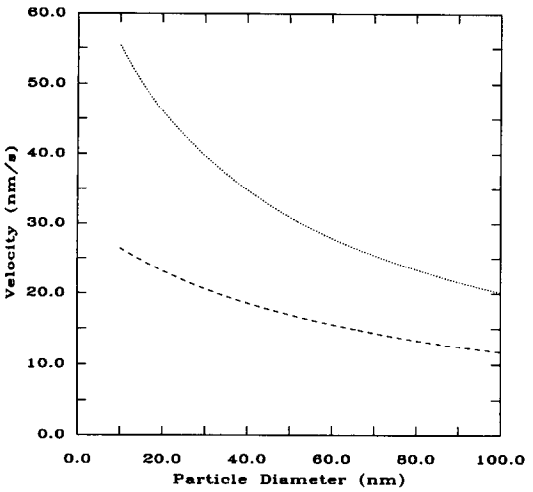

FIG. 4. Effect of channel depth on particle velocity for $L/2R = 1$. (---) $L_c/L = 0.5$ or 50% coverage; (· · ·) $L_c/L = 0.25$ or 25% coverage.

neling velocity depends not only on the particle diameter but also on the aspect ratio and the percentage of particle-covered area. As a result, virtually any experimental point can be reproduced by adjusting them.

The larger the percentage of particle-covered area the more carbon must diffuse through the particle reducing the channeling velocity as shown in Figs. 4 and 5. The fact that indeed the particle velocity is inversely proportional to the channel depth especially for small particles can be observed from Table 2. It was found that catalytic particles of 10 nm diameter with channel depth one-fourth of their height (25% coverage) translate twice as fast as particles of the same size but with twice the channel depth (50% coverage). However, for larger particles, e.g., 50 nm diameter, doubling the coverage decreases the linear velocity by a factor of 1.8 only. Furthermore, the larger the aspect ratio with constant percentage of covered area the larger is the slope of the curves in Fig. 3 for small particles.

On the other hand, when the channel depth is the same for particles of increasing

TABLE 2

Relation between Percentage Coverage and Velocity for Different Particle Diameters, $L/2R = 1$ and $k = 2.52 \times 10^{-4}$ cm/s

Diameter (nm)	$V_{25\%}$ (nm/s)	$V_{50\%}$ (nm/s)	$V_{25\%}/V_{50\%}$
10	55.37	26.44	2.094
20	46.14	23.16	1.992
50	30.92	16.92	1.827
100	20.13	11.73	1.716

diameters the velocity increases as shown in Fig. 6 for a constant channel depth of 5 nm. Here the effect on the velocity of decreasing the percentage of covered area is more pronounced than the retarding effect of a longer diffusion path associated with larger particles. However, one cannot rule out the fact that under different operating conditions, the effect of the smaller particle may become predominant. In the upper curve of Fig. 6 the same value of the reaction rate constant was used. However, that resulted in a linear velocity for a 52-nm-diameter particle that was 3.8 times the velocity of a similar particle in a channel of depth 25 nm. In order to achieve agreement

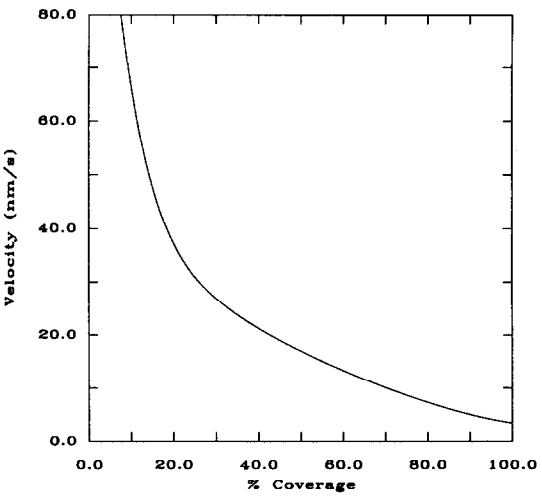

FIG. 5. Effect of channel depth on particle velocity for a single particle size of $L = 2R = 50$ nm.

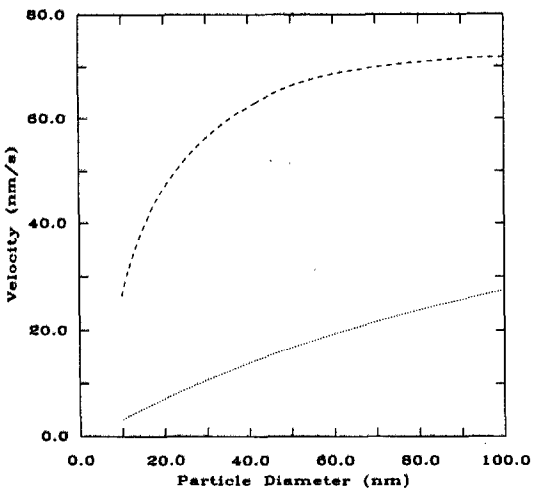

FIG. 6. Effect of reaction rate constant on particle velocity for a particle aspect ratio $L/2R = 1$ and channel depth $L_c = 5$ nm. (---) $k = 2.52 \times 10^{-4}$ cm/s; (· · ·) $k = 2.7 \times 10^{-5}$ cm/s.

with the experimental results and a channel depth of 5 nm one would have to assume a reaction rate constant that is one order of magnitude smaller as shown in the lower curve in Fig. 6.

Next the reduction of graphite with H_2 over Ni is examined under the conditions summarized in Table 3. The values for diffusivity and solubility of carbon in Ni in the temperature range 700°–1300°C have been reported by Lander *et al.* (*12*). It is anticipated that the C–H_2 reaction will be slower than carbon oxidation, in accordance with some of the results of Baker and Sherwood (*5*) and Keep *et al.* (*6*). However, the channeling velocities reported by the former researchers during oxidation are significantly smaller than those during reduction (see their Figs. 1 and 8). A number of reasons can be presented to explain this behavior (e.g., formation of NiO during oxidation which retards carbon diffusion). It was thus decided to compare the predictions of the present model with the results of Keep *et al.* They reported that channeling of four different particles at 1035°K resulted in a constant gasification rate per particle surface area (see their Table 2).

In a procedure similar to that reported in their appendix, we calculated a reaction rate constant using one of their data points and assuming that carbon concentration is equal to carbon solubility throughout the particle. The result was $k = 3.31 \times 10^{-6}$ cm/s and indeed this is much lower than the corresponding value for carbon oxidation on Pd, although the solubilities and diffusivities of carbon in these two metals are not too different (compare Tables 1 and 3). Therefore, it is possible that in a reducing environment the channeling action is no longer controlled by diffusion of C in the catalyst. Using this value the channeling velocity was predicted for different sizes of channeling particles and channel depths. As seen in Fig. 7, the channeling velocity is not affected by the particle diameter. This verifies that this process is controlled by the reaction kinetics, since the amount of carbon reacted is proportional to the exposed catalytic surface. However, the channeling velocity is still inversely propor-

TABLE 3

Physicochemical and Geometrical Parameters Used for C Reduction over Ni

Diffusivity	$D = 2.48 \exp\left(-\frac{20{,}200}{T}\right) \frac{\text{cm}^2}{\text{s}} \left(8.29 \times 10^{-9} \frac{\text{cm}^2}{\text{s}} \text{ at } 1035 \text{ K}\right)$
Solubility	$C_0 = 1.05 \exp\left(-\frac{4{,}880}{T}\right) \frac{\text{g}}{\text{cm}^3} \left(0.0094 \frac{\text{g}}{\text{cm}^3} \text{ at } 1035 \text{ K}\right)$
Particle diameter	$10 \text{ nm} \leq 2R \leq 100 \text{ nm}$
Ratio of particle height to diameter	$L/2R = 1$
Ratio of channel depth to particle height	$L_c/L = 0.25, 0.5$, and 1

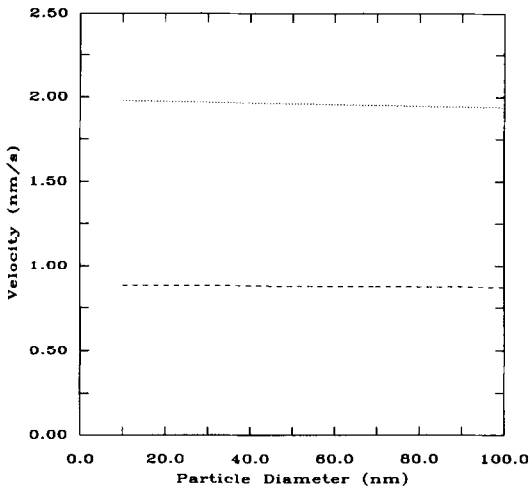

FIG. 7. Effect of particle size on particle velocity for two different channel depths during graphite gasification by H_2.

tional to the channel depth. In addition, in a reducing environment the catalytic particles translate much more slowly than they do in an oxidizing environment since they have to overcome the slower surface reaction step in addition to the diffusion step which remains approximately the same (compare particle velocities in Figs. 6 and 7).

Finally, the present model predicts a gasification rate per surface area for reaction that does not depend on the particle size. The predicted value is 0.139 nm/s and compares very well with that reported by Keep *et al.* which is 0.141 nm/s.

CONCLUDING REMARKS

The proposed model for catalytic gasification of graphite can be used when the overall gasification mechanism is controlled by either carbon diffusion through the catalyst or surface reaction of carbon with H_2. In both cases it provides a powerful predictive tool. It has indeed demonstrated that when the diffusion step is rate controlling and if the aspect ratio and particle coverage are the same, the particle velocity is inversely proportional to the particle size for relatively small particles. Moreover, when the reaction step is rate controlling the amount of carbon gasified per exposed area of particle remains constant. Finally, this work suggests that there is a strong need for further development of the experimental procedure so that both the particle shape and dimensions and the channel depth can be measured *in situ* along with the channeling velocity.

ACKNOWLEDGMENTS

This work was partially supported by NSF Grant MSM-8705735. The authors are grateful to C. R. F. Lund and R. T. Yang for valuable discussions concerning this work. The constructive comments of an anonymous referee are gratefully acknowledged. Part of the computations were performed at the Cornell National Supercomputing Facility.

REFERENCES

1. Walker, P. L., Jr., Shelef, M., and Anderson, R. A., *Chem. Phys. Carbon* **4,** 287 (1968).
2. McKee, D. W., *Chem. Phys. Carbon* **16,** 1 (1981).
3. Baker, R. T. K., France, J. A., Rouse, L., and Waite, R. J., *J. Catal.* **41,** 22 (1976).
4. Baker, R. T. K., *Catal. Rev. Sci. Eng.* **19**(2), 161 (1979).
5. Baker, R. T. K., and Sherwood, R. D., *J. Catal.* **70,** 198 (1981).
6. Keep, C. W., Terry, S., and Wells, M., *J. Catal.* **66,** 451 (1980).
7. Goethel, P. J., and Yang, R. T., *J. Catal.* **101,** 342 (1986).
8. Choi, A. S., Devera, A. L., and Hawlay, M. C., *J. Catal.* **106,** 313 (1987).
9. Holstein, W. L., and Boudart, M., *Lat. Amer. J. Chem. Eng. Appl. Chem.* **13,** 107 (1983).
10. Goethel, P. J., Tsamopoulos, J. A. and Yang, R. T., *AIChE J.*, **35**(4), 686 (1989).
11. Goethel, P. J., Ph.D. dissertation, State University of New York, Buffalo, 1988.
12. Lander, J. J., Kern, H. E. and Beach, A. L., *J. Appl. Phys.* **23**(12), 1305 (1952).